Application of Euler Deconvolution and Forward Modelling Techniques in Estimating Depth to Magnetic Structure in Lake Baringo Area, in the Kenyan Rift.

Seurey.P[1], GithiriJ.G.[2], AmbussoW. J.[3]

[1,3]Kenyatta University, Physics Department, P.O BOX 43844, Nairobi- Kenya
[2]Jomo Kenyatta University of Agriculture and Technology, Physics Department, P.O BOX 62000, Nairobi – Kenya

Abstract: *Ground magnetic survey was carried out in the study area with the aim of locating depth estimates to bodies with sufficient magnetic susceptibility contrast that may represent magmatic intrusions. The magnetic data was corrected, a total magnetic intensity contour map produced and profiles drawn across discerned anomalous regions.Two dimensional (2D) Euler deconvolution was applied on the selected profiles of reduced ground magnetic data. Geologic constraint was imposed by use of a structural index of 1.0 that best describes prismatic bodies like intrusive sills and dykes. 2D Euler solutions revealed subsurface faulting activities and the presence of fluid-filled zones within the survey area which are marked by the absence of magnetic sources. The magnetic bodies were imaged at variable depths ranging from the surface to about 0.5km. These depth estimates were later used as start-up parameters for 2D- forward modeling using 'Mag2DC' computer program.The average modeled depth for the near surface magnetic anomaly sources of the area is 86.57m, while that of the deep seated anomaly sources is 349.25m. The bodies display susceptibility as high as 0.5301 SI units to as low as –0.841 SI units. The models show extensive lava flows. They are suggested to be basaltic sills and dykes of different types based on geologic unit of the area. They may be possible heat source causing a thermal anomaly in the area west of Lake Baringo and such may have been magmatic intrusive that remained at the subsurface.*
Keywords: *Magnetic, Euler Deconvolution, Forward modeling, Baringo*

I. Introduction

Lake Baringo prospect area is located within the eastern floor of the Kenyan rift valley, which is part of the East African Rift System. It is bounded by latitudes 0^0 30'N and $0^0$45'N and longitudes 35^059'E and 36^0 10'E as illustrated in figure 1. It is one of the important areas on the Kenyan rift floor that are associated with possible occurrence of geothermal resource. The Tugen hills, an uplift fault block of volcanic and metamorphic rocks lies west of the lake. The Laikipia escarpment lies to the east. Lake Baringo Geothermal Prospect is one of the several important areas on the Kenya Rift floor that are associated with possible occurrence of geothermal resource. The Kenya Rift valley is a prominent feature of geographic and geologic interest. The rift is developed within a stable orogenic belt that skirts around a craton. Several Tertiary volcanoes on its floor mark the Kenya portion of this rift. Some areas in the Kenya Rift are dotted with hydrothermal activity and are envisaged to host geothermal systems.

Hydrothermal activity in the Lake Baringo prospects is manifested by extensive occurrence of fumaroles, hot spring, altered grounds and thermally anomalous ground-water boreholes. One of these boreholes, the Chepkoiyo borehole, which was drilled in April 2004, self-discharged water at 98°C (local boiling point). The chemistry of the discharged fluids indicated possible input from a geothermal reservoir.
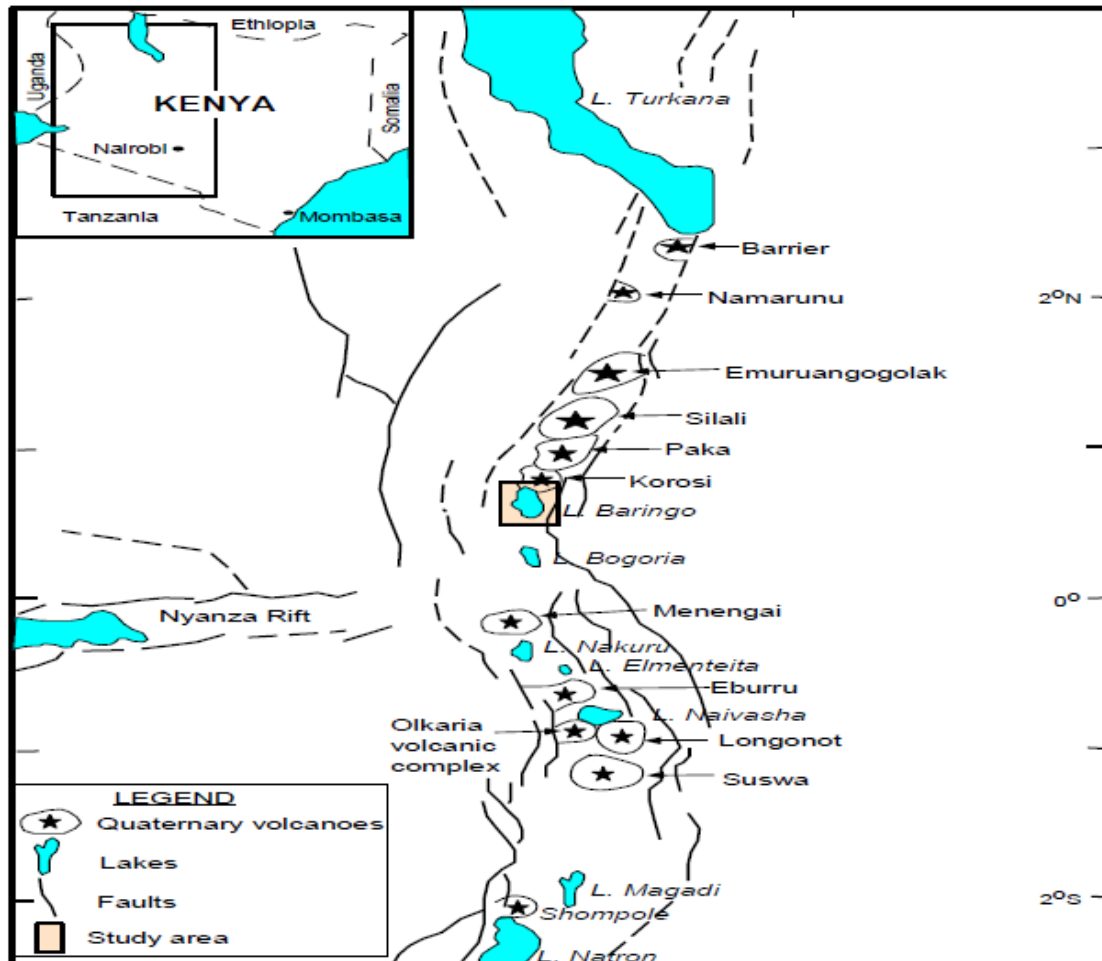
Figure 1: Location of the Lake Baringo Geothermal Prospect in the Kenya Rift

II. Geologic Setting

The geology of the area is dominated by intermediate lavas (trachytes and trachy-phonolites) in the west and east sectors of the prospect area and basalts in the north. The southern sector is, however, dominated by fluvial and alluvial deposits. The Baringo trachyte was described by Martyn (1969) as the 'Lake Baringo Trachyte'. The Baringo trachyte outcrops over 12km^2 west of KampiyaSamaki. It was the major source material for artifacts found in Kapthurin basin (Tallon, 1978). The striking appearance on aerial photographs is due to lineaments which reflect pressure ridges resulting from the congealing of highly viscous lava. The trachyte is fine grained, black, streaked with green and locally speckled, an expression of glomerophyric clusters of dark minerals. Sanidine forms about 60% of the mode: otherwise aegirine-angite, aenigmatite and zeloilites are commonly observed in this section (Dagley et al ,1978).Thin basalt flows occur on the west side of the lake (Truckle, 1977) forming the greater part of the outcrops which (Martyn 1969) reffered to 'Basalts of Nginyang type'. They are well exposed on the lake shores promontories between Kampi ya Samaki and west Bay, and further north at Logoratibim. The Baringo basalts typically weather black with a rough texture due to vascularity. Columnar or rough blocky jointing is usual. The lake has several small islands, the largest being Olkokwe island which is an extinct volcanic center related to Korosi volcano, north of the lake. The chemistry of the discharged fluids indicates possible input from a geothermal reservoir. Figure 2 shows the geologic map of Lake Baringo geothermal prospect.
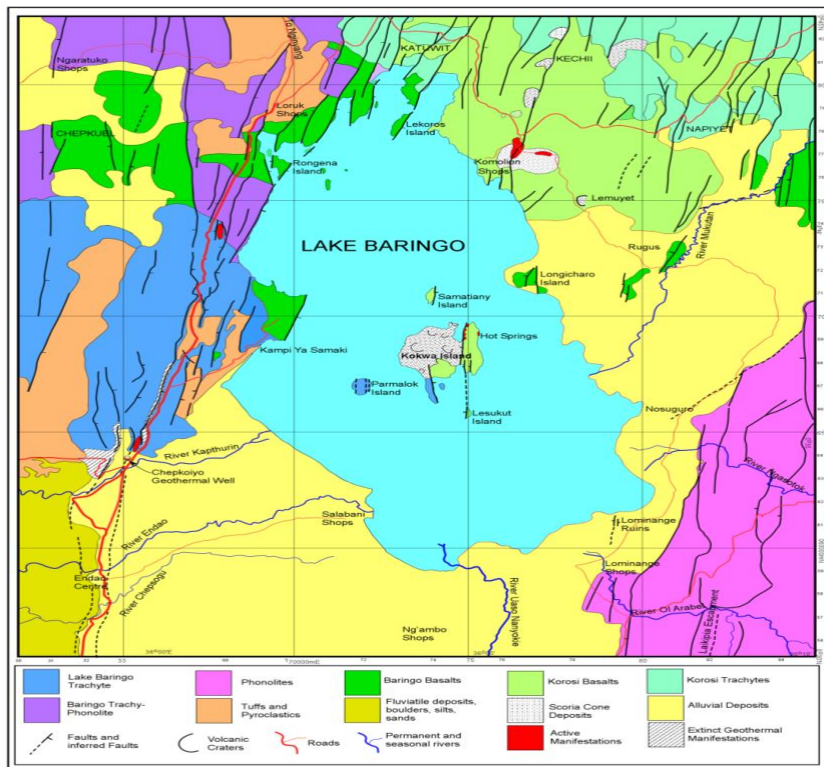
Figure 2: Geological map of the lake baringo geothermal propect (Dunkley et al 1993)

III.   Methodology

The field stations were selected carefully along a profile in the study area and were positioned using Global Positioning System (GPS). The profile and station separation was set at about 800m and 500m respectively. The vertical magnetic field intensities were then measured using Flux Gate magnetometer. Data reduction was done to correct for diurnal and geomagnetic variations. Surfer 8.0 software was then used for gridding and to plot contour map to establish the anomaly signature of the area. Profiles were selected from total magnetic intensity contour map passing through discerned anomalies. Figure 3 shows reduced vertical magnetic intensity contour map and selected profiles.
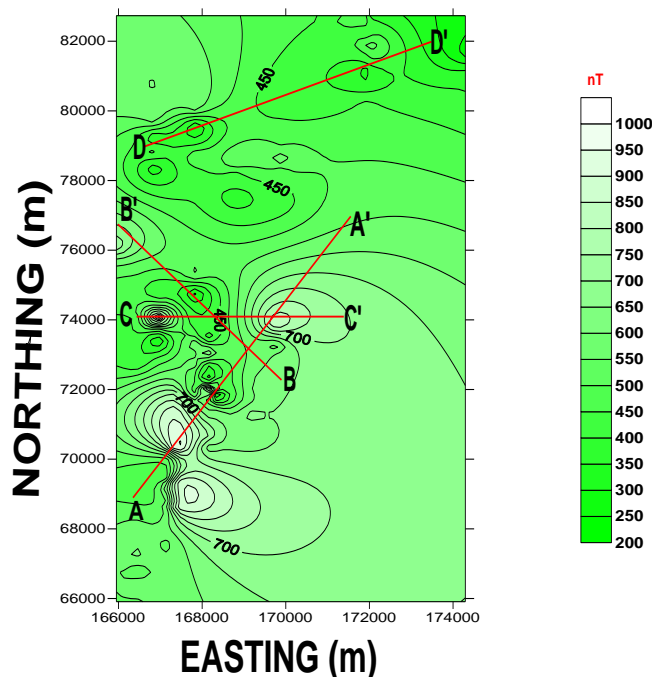

Figure: 3 Vertical magnetic intensity contour map with the selected profiles

3.1 Euler deconvolution

Euler deconvolution is a data enhancement technique for estimating location and depth to magnetic anomaly source. It relates the magnetic field and its gradient components to the location of the anomaly source with the degree of homogeneity expressed as a structural index and it is a suitable method for delineating anomalies caused by isolated and multiple sources (ElDawi et al., 2004). Euler deconvolution is expressed in Equation 3.1as:

$$(x - x_0)\frac{\partial T}{\partial x} + (y - y_0)\frac{\partial T}{\partial y} + (Z - Z_0)\frac{\partial T}{\partial Z} = n(B - T) \quad 3.1$$

Applying the Euler's expression to profile or line-oriented data (2D source), x-coordinate is a measure of the distance along the profile and y-coordinate is set to zero along the entire profile. Equation 3.1 is then written in form of Equation 3.2 as:

$$(x - x_0)\frac{\partial T}{\partial x} + (Z - Z_0)\frac{\partial T}{\partial z} = n(B - T) \quad 3.2$$

Where (x_0, z_0) is the position of a 2D magnetic source whose total field *T* is detected at (x, z) . The total field has a regional value of *B,* and *n* is a measure of fall -off rate of the magnetic field. *n* is directly related to the source slope and is referred to as the structural index and depends on the geometry of the source (El Dawi et al., 2004). Estimating depth to magnetic anomaly using Euler deconvolution involves:

i)   Reduction to the pole and
ii)   Calculation of horizontal and vertical gradients of magnetic field data, calculated in frequency domain,
iii) choosing window sizes
iv) Structural index, e.g. contact and dyke.

Table 1 displays structural indices for different possible geological structures.

Table 1: Structural indices for different geological structures (after Reid etal. 1990)

Structural index	Geologic Structure
0	Contact
0.5	Thick step
1	Sill / Dyke
2	Vertical pipe
3	Sphere

The input data to the software was profile magnetic data. For the magnetic Euler solutions other than profile data, other input information included magnetic inclination, declination and the background normal total magnetic field. Magnetic declination of value 1.145^0 was used for the study area as from topographic map sheet 91/3 printed by survey of Kenya. By qualitative interpretation of the magnetic contour map's quiet areas, a normal total vertical magnetic field was approximated as11300 nT. The magnetic inclination of -19.567^0 of the study area was also imputed.

The results of the International Geomagnetic Reference Field (IGRF) are given in the table 2 below.

Table 2: IGRF components of Lake Baringo area

Component	Field Value
Declination	1.145^0
Inclination	-19.567^0
Total vertical Intensity	11300 nT

3.2 Reduction to the Pole

This simplifies the interpretation of anomalies by removing the symmetry introduced due to its induction by the inclined main field. The main field is only vertical (and induced anomaly symmetric) at the north and south magnetic poles. In reduction to the pole procedure, the measured total fieldanomaly is transformed into the vertical component of the field caused by the same sourcedistribution magnetized in the vertical direction. The acquired anomaly is therefore the onethat would be measured at the north magnetic pole, where induced magnetization andambient field both are directed downwards (Blakely, 1995).The software Euler was used in reducing to the pole the magnetic profile data. This was important for outlining magnetic units and positioning magnetic discontinuities, which may correspond to faults. Reduction to the pole is usually unreliable at low magnetic latitudes, where northerly striking magnetic features have little magnetic expression. Some bodies have no detectable magnetic anomaly at zero inclination (Blakely, 1995). The validity of the reduction to the pole is doubtful for inclinations lower than approximately 15º. The average inclination in the survey area was -19.567º and therefore reduction to the pole was considered reliable.

3.3 Boundary analysis by vertical and horizontal gradients

This quantifies the spatial rate of change of the magnetic field in vertical or horizontal direction. Derivatives essentially enhance and sharpen high frequency anomalies to low frequencies. This numerical filtering method is effective in enhancing anomaly due to shallow sources; it narrows the width of anomalies and very effective in locating source bodies and defining the boundaries of magnetic bodies.

IV.   Results And Discussion

4.1 Euler solutions

Figure 4 shows Euler solutions for magnetic anomaly along profile AA'. From magnetic profile AA' in fig 5.3, calculated solutions map the depth to the subsurface structure. A structural index of 1.0 was used since it best represents sill edge, dike, or fault. The horizontal and vertical gradients fluctuate at a distance of 1.5 km to 2.0 km, 3.5 km 4.0 km and at 5.5 km. This may represent abrupt lateral change in magnetization over the distance range.There is relatively low magnetic anomaly signature along the profile at 0 -1 km and 4 km -5.5 km. The shoulder of RTP curves within these ranges outlines the edges of possible faults and evidence of the presence of the fluids. The depth to the magnetic structure is approximately 0.6 km.
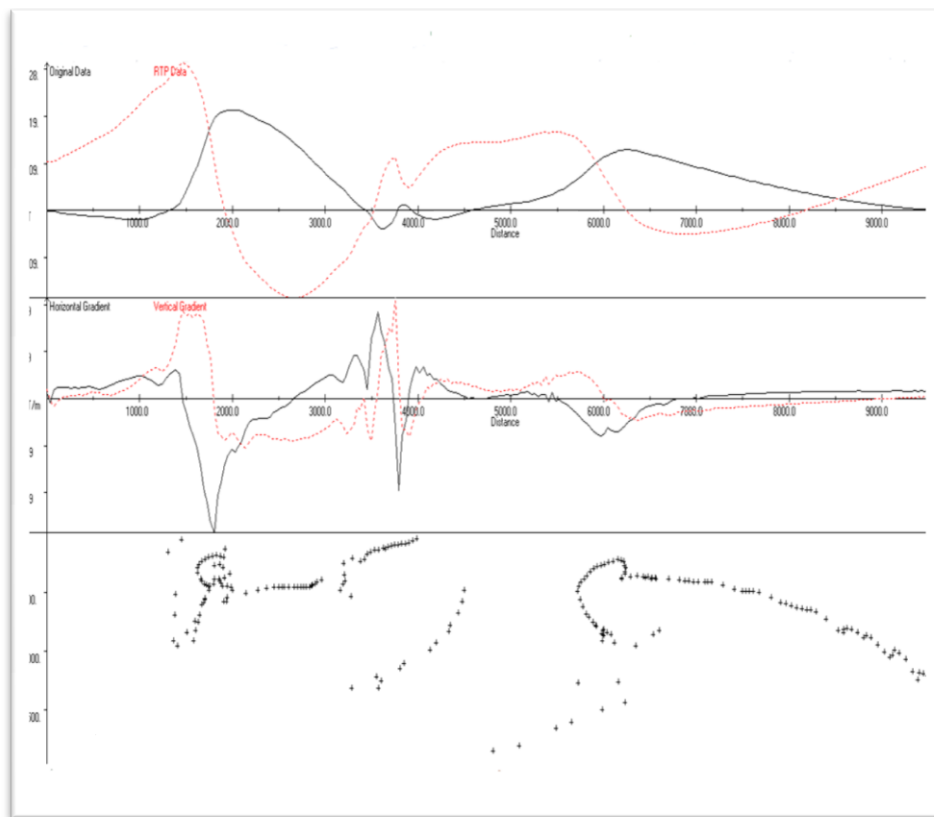

Figure 4: Euler depth solutions along magnetic anomaly profile AA'

From magnetic profile BB' in figure 5, Euler solution cluster is observed at 1.5 km and at 2km.There is an abrupt change in both horizontal and vertical gradients at 1.8 and at4.5 km profile distance. At the same location the shallowest depth of approximately 50 m is attained.
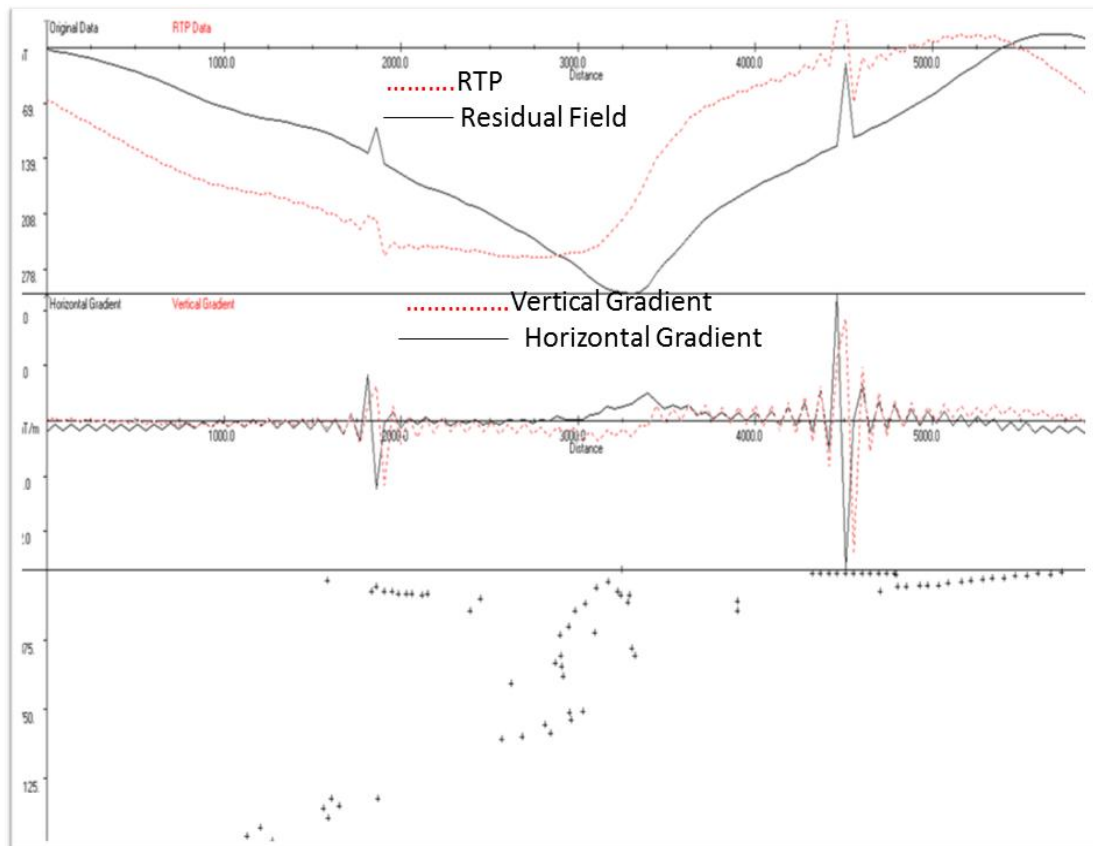

Figure 5: Euler depth solutions along magnetic anomaly profile BB'

From the magnetic profile CC' in fig 6 the Euler solution have the shallowest depth at 250m and the deepest at 750m. The RTP curve display a magnetic high at 500m and at 3250m and a magnetic low at 1500m which represent rocks of high and low magnetic susceptibility respectively relative to the host rocks. Abrupt changes in horizontal and vertical gradients at 400m indicate possible change in magnetization.
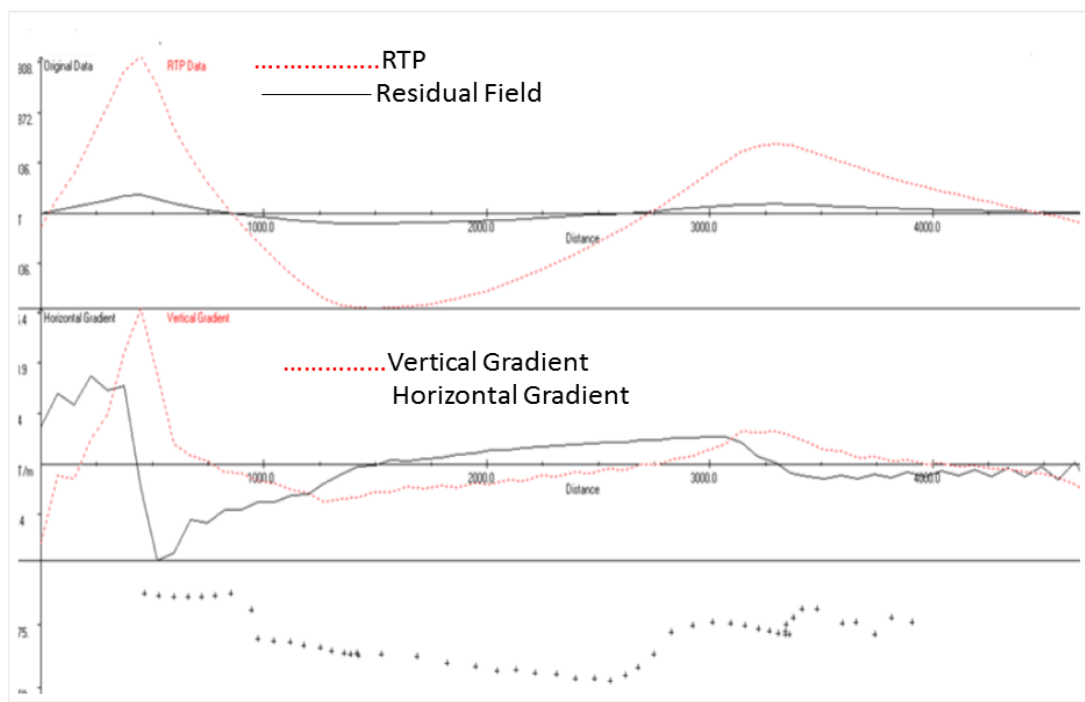

Figure 6: Euler depth solutions along magnetic anomaly profile CC'

The Euler magnetic analysis along profile DD' in figure7 reveals a magnetic structure to a maximum depth of approximately 0.5 km. The RTP curve has a magnetic high at 1.75 km and at 5.75 km which could be indicative of the edges of the causative bodies. The horizontal and vertical gradients fluctuate at a profile distance of 1.25km and 5.5km which are also the points of inflection of RTP.This suggests the top of a magnetic body.
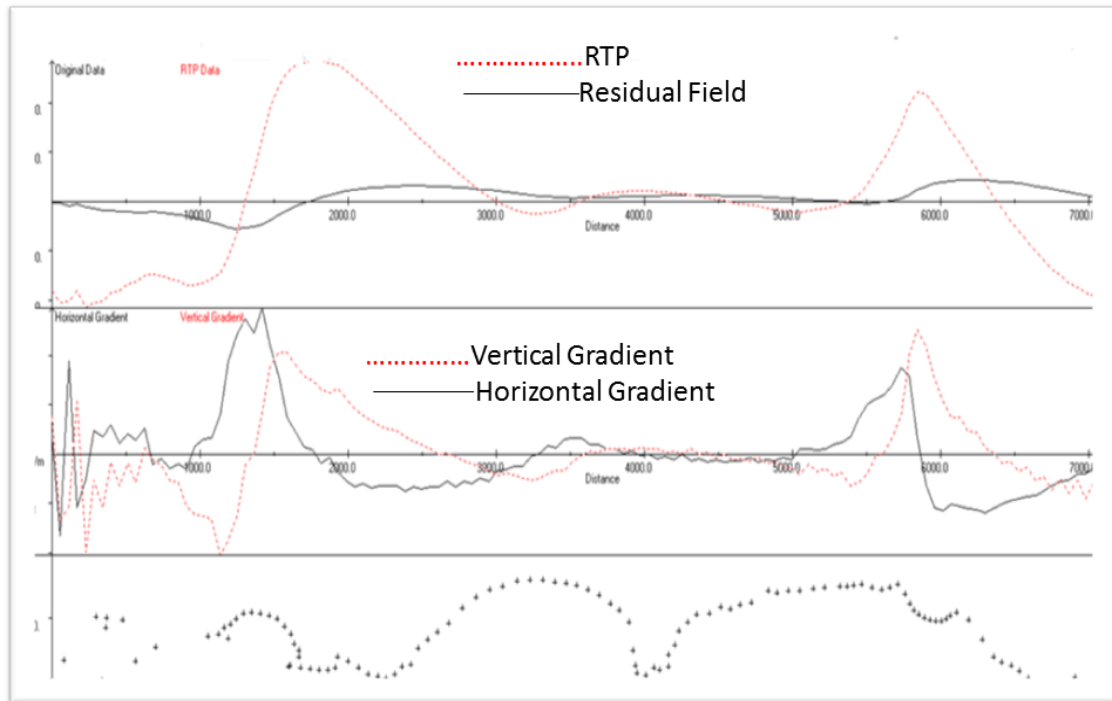

Figure7: Euler depth solutions along magnetic anomaly profile DD'

4.2 2D Forward modeling

Forward modelling was done using mag2dC computer program. 'mag2dC' calculates the anomalous field caused by an assemblage of 2–D magnetic bodies defined by a polygonal outline. Mag2dc for Windows allows the forward modelling and inversion of magnetic data The use of this program involves a trial and error procedure to obtain a good fit to the observed anomalies. Geophysical constrains like known surface geology are also imposed because of ambiguity in magnetic data. Figures 8 to 11 show the modelled bodies of the subsurface geological structures causing anomalies on the selected profiles.
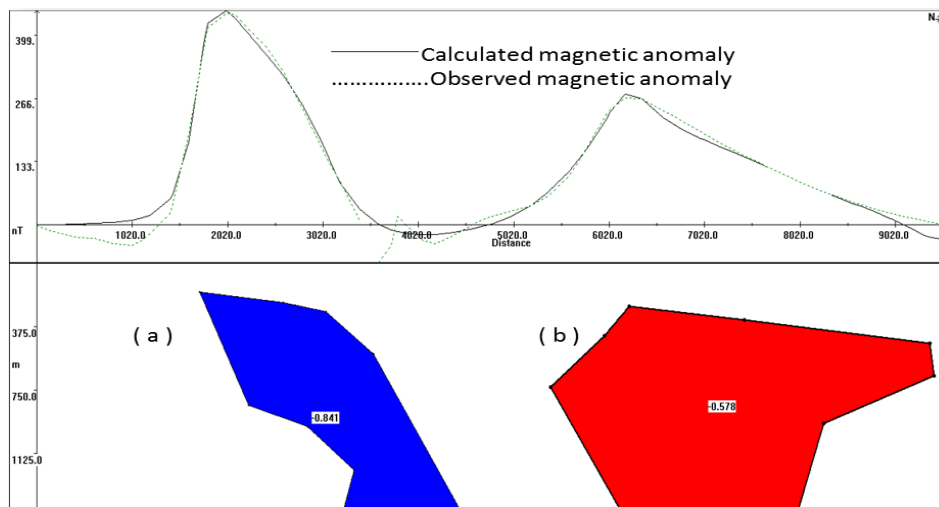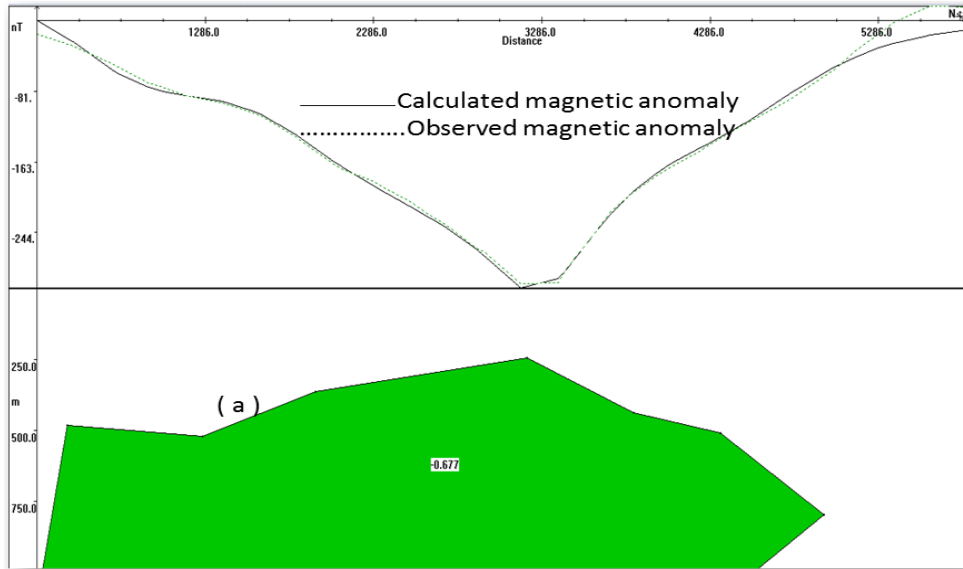

Figure 8: magnetic model along profile AA'

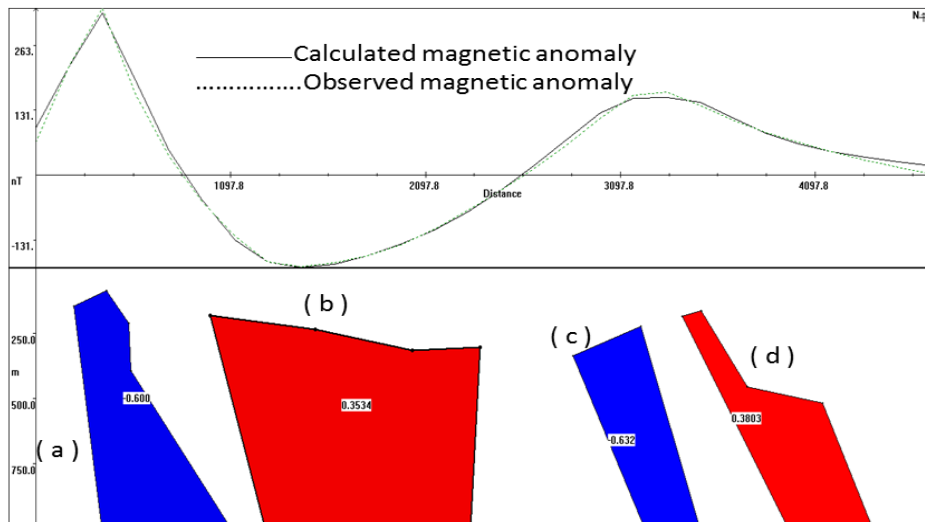**Figure 9:** magnetic model along profile BB'

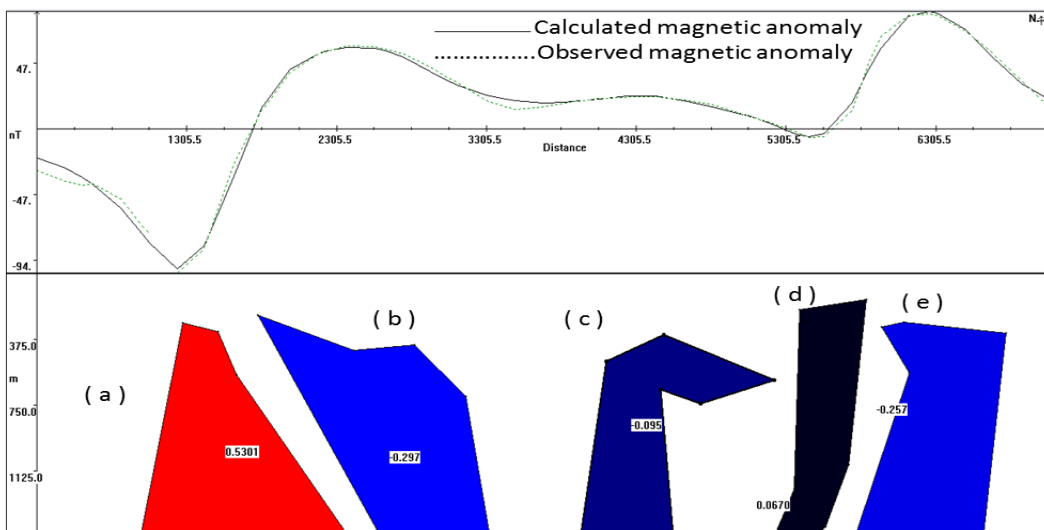**Figure 10:** magnetic model along profile CC'

Figure 11: magnetic model along profile DD'

The results of the model parameters of the causative bodies as determined by forward modelling are shown in Table 3.

Table 3: Modelled parameters of the causative bodies

Profile name	Causative bodies	Modeled depth, a, (m)	Modelled susceptibility, k, (SI)
AA'	a	170.15	-0.841
	b	255.23	-0.578
BB'	a	244.78	-0.677
CC'	a	86.57	-0.600
	b	182.09	0.353
	c	223.88	-0.632
	d	164.18	0.3803
DD'	a	228.09	0.5301
	b	237.313	-0.297
	c	349.25	-0.095
	d	147.07	0.067
	e	277.61	-0.257

4.2.1 Models interpretations

Profile AA' in magnetic intensity map cuts across a high magnetic signature region towards SW and a low magnetic signature region towards the NE. It therefore trends in the direction NE-SW.Models in profile AA' show two subsurface magmatic intrusive bodies which are postulated to be basaltic sills and basaltic dykes forming along the fracture zones. At a distance of 2022m and 6020m along the profile correspond to magnetic highs, and a basaltic dyke and basaltic sill form at depths of 170m and 255m from the surface and their susceptibilities are -0.841 and -0.578 SI respectively.

Profile BB' trends NE-SE in the magnetic intensity map. It has a magnetic low at a distance of 1597m along the profile. The model on profile BB' suggests a body at a depth of 245m from the surface. This is postulated to be a magmatic intrusive, and more likely to be a basalt sill. Its magnetic susceptibility is –0.677 SI.

The magnetic model along profile CC' illustrated by fig. 5.9 has two magnetic highs at 250m and 3348m along the profile. At these points modeled bodies are at depths of 87m, 224m and 164m while their magnetic susceptibilities are -0.600 SI,-0.632 SI and 0.3803 SI respectively. These bodies are suggested to magmatic intrusive, likely to be basaltic dykes. At a distance of 1598m along the profile is a magnetic low. The modeled body at this point is a horizontal magmatic intrusive of depth 182m and magnetic susceptibility of 0.353 SI. It is suggested to be a volcanic sill formed along the fractures zones because of its orientation.

Profile DD' is on the northern region of the magnetic intensity map. It trends in the direction NEE-SWW in the study area. On this profile, five bodies of different magnetic susceptibility, depth and geometry are modeled. They are magmatic intrusive arising from extensive lava flow. They are suggested to be dykes.

V.   Conclusion

In this study, the magnetic prospecting method was found to be effective in detecting subsurface causative bodies postulated to be heat sources rooted from the asthenosphere.Simple magnetic bodies of prismatic shapes were modeled assuming uniform magnetization higher the surrounding rock. The confidence level in the resultant model was depended not only on the degree of fit but also geophysical constrains imposed during modeling. The visual inspection and analysis of the magnetic intensity map, discontinuities in Euler solution cluster along the profiles and the models revealed that Lake Baringo prospect area is generally characterized by broad and low magnetic signatures at the western and north western parts.

The average modeled depth for the near surface magnetic anomaly sources (postulated to be a basaltic dyke) of the area is86.57m, while that of the deep seated anomaly sources is 349.25m. The ground magnetic study of this area has helped to delineate lineaments and target zones with magmatic intrusives. The major subsurface structures delineated (faults/fractures, sills and dykes) will aid the geothermal exploration work in the area.Also, the near linear nature of the anomalies in this prospect area suggests that the rocks may be bounded by faults.The results further support the delineation of faults/fractures and heat sources associated with shallow intrusive along structures. Indeed it is in agreement with the resistivity findings and results of previous geophysical measurements that the Baringo prospect appears to host a geothermal system on the western side of Lake Baringo. Major structures like faults NE-SW along the rift floor tend to strongly influence the resistivity distribution in the area.

Acknowledgement

References

[1]. Blackely, R.J. (1995). *Potential theory in gravity and magnetic application* **70**: 285-303 Dagley,P.,Mussette, A. F. and Palmer,H.M. (1978), *Preliminary observations on the palaeomagnetic stratigraphy on the area west of Lake Baringo, Kenya*.225-235 in Bishop,w.w (Editor),q.v.

[2]. Dunkley, P.N., Smith, M., Allen, D.J., and Darling, W.G.(1993). *The geothermal activity and geology the northern sector of the Kenya Rift Valley.British Geological Survey (BGS) Research Report, SC/93/1.*

[3]. El Dawi, M.G., Tianyou, L., Hui, S. and Dapeny, L. (2004). *"Depth estimation of 2-D magnetic anomalous sources by using Euler deconvolution method."* American Journal of Applied Sciences.

[4]. Marty, J.E. (1969).*The geological history of the country between Lake Baringo and the Kerio river, Baringo district, Kenya*,PhD. Thesis University of London 228 ppc.

[5]. Reid, A.B., Allsop, J.M., Granser, H., Millett, A.J. and Somerton, I.W. (1990). "*Magnetic interpretation in three dimensions using Euler deconvolution.*"Geophysics, 55, 80-91.

[6]. Tallon, P.W.J. (1978*). Geological setting of the hominid fossils and Acheulianartifacts from the Kapthurin formation, Baringo district, Kenya.* 361-173.

[7]. Truckle, P.H. (1977).*Geological map of Lake Baringo-Laikipia area, Directorate of overseas surveys, ordnance survey.*